MODELLING THE INFLUENCE OF COMPOSITE STIFFNESS ON ENERGY DISSIPATION IN REINFORCED COMPOSITE CONCRETE FLOORS

K. GROMYSZ[1]

A continuous contact layer exists between the top and bottom layer of concrete composite reinforced floors. The contact layer is characterised by linear elasticity and frictional properties. In this paper a model of single degree of freedom of composite floor is determined. The model assumes that the restoring forces and the non-conservative internal friction forces dissipating energy are produced within the contact layer. A hysteresis loop is created in the process of static loading and unloading of the model, with the energy absorption coefficient being defined on this basis. The value of the coefficient is rising along with the growing stiffness of the composite.

A critical damping ratio is a parameter describing free decaying vibration caused by non-conservative internal friction forces in the contact layer and in the bottom and top layer. The value of the ratio in the defined model is rising along with the lowering stiffness of the element representing contact layer.

The findings resulting from the theoretical analyses carried out, including the experimental tests, are the basis for the established methods of determining the concrete layer state for reinforced concrete floors. The method is based on energy dissipation in the contact layer.

Key words: reinforced concrete floors, composite structures, internal friction, energy dissipation, free vibrations.

1. BASIC NOTATION

Below are the most important notations referring to the stiffness and energy dissipation parameters in the models presented in the paper and in real structures:

$c_{q,w}$	–	damping coefficient in model of the continuous contact layer,
$c_{Q,w}$, $c_{Q,m}$, $c_{Q,w,m}$	–	damping coefficient in model of single degree of freedom, taking into account internal friction in: contact layer, monolithic floor, entire model of composite floor,
$k_{q,w}$	–	stiffness of the contact layer, determined experimentally, is an equivalent to the resultant stiffness $k_{q,w,x}$
$k_{q,w,el}$, $k_{q,w,fr-int}$,	–	stiffness of element in a model of the continuous contact layer representing: linear and elastic properties, elastic and frictional properties,

[1] Ph.D., Silesian University of Technology, Department of Building Constructions, Gliwice, Poland, e-mail: krzysztof.gromysz@polsl.pl

$k_{q,w,z}$, $k_{q,w,x}$	–	substitute stiffness element under growing load, resultant stiffness element in a model of the continuous contact layer,
$k_{Q,m}$	–	stiffness of the monolithic concrete floor at the point*, determined experimentally on the basis of hysteresis loop is equivalent to the resultant stiffness $k_{Q,m,x}$,
$k_{Q,m,el}$, $k_{Q,m,fr-int}$	–	stiffness of monolithic floor in model of single degree of freedom representing: linear and elastic properties, linear and frictional properties,
$k_{Q,m,z}$, $k_{Q,m,x}$	–	stiffness of monolithic floor in model of single degree of freedom: substitute stiffness, resultant stiffness,
$k_{Q,w}$	–	component stiffness of composite concrete floor at the point*,
$k_{Q,w,el}$, $k_{Q,w,fr-int}$	–	component stiffness of composite concrete floor in model of single degree of freedom modeling: linear and elastic properties, linear and frictional properties,
$k_{Q,w,z}$, $k_{Q,w,x}$	–	stiffness in model of single degree of freedom of composite concrete floor: component of substitute stiffness, component of the resultant stiffness,
$k_{Q,w,m}$	–	stiffness of composite concrete floor at the point*; determined experimentally on basis of hysteresis loop is equivalent to the resultant stiffness $k_{Q,w,m,x}$,
$k_{Q,w,m,x}$	–	resultant stiffness of the composite concrete floor model of single degree of freedom,
$\chi_{q,w}$	–	energy absorption coefficient in element of a model of the continues contact layer,
$\chi_{Q,m}$, $\chi_{Q,w,m}$	–	energy absorption coefficient determined experimentally at the point* during tests: monolithic concrete slab, composite concrete slab,
$\psi_{q,w}$	–	hysteresis loop area of element in model of a continues contact layer,
$\psi_{Q,m}$, $\psi_{Q,w,m}$	–	hysteresis loop area of model of single degree of freedom of: monolithic concrete slab, composite concrete slab,
$V_{q,w}$	–	the smallest area of a rectangle into which the loop of area $\psi_{q,w}$ can be inscribed,
$V_{Q,m}$, $V_{Q,w,m}$	–	the smallest area of a rectangle into which the loops of area $\psi_{Q,m}$ and $\psi_{Q,w,m}$ can be inscribed,
ζ_m, $\zeta_{w,m}$	–	damping ratio of first vibration form of: monolithic floor, composite floor

* the point is meant as a point on the floor of the abscissa where the antinode of the first vibration form appears.

The parameters to be experimentally determined during the tests carried out on composite and monolithic floors include: $k_{q,w}$, $k_{Q,m}$, $k_{Q,w,m}$, $\chi_{Q,m}$, $\chi_{Q,w,m}$, ζ_m, $\zeta_{w,m}$. The value of the other parameters can be determined based on the parameter values identified in the tests.

2. Introduction

Composite reinforced concrete floors consist of two layers of concrete: a bottom layer being a precast element, and a top layer produced on site. It has been assumed that the contact layer exists between the layers, and forces are induced in the contact layer connected with elastic and inelastic strains.

The results of the experimental investigations reveal [1] that if the contact layer is stiff and does not permit the displacement of the bottom layer in relation to the top layer, by the value greater than w_{gr} of approx. 0.1 mm, the composite is balancing the longitudinal shearing forces τ_{sj}. The following are responsible for balancing such forces: conservative forces that are not dispersing the energy and are connected with the elastic strains of the vertical reinforcement, and with the elastic strains of the contact concrete layer, as well as non-conservative forces dispersing the energy connected with internal friction, occurring within the material of contact layer. The continuity of contact layer strains is maintained in this phase of the structure's work and elastic and inelastic strains are present in both, the process of loading and unloading of the slab (Fig. 1).
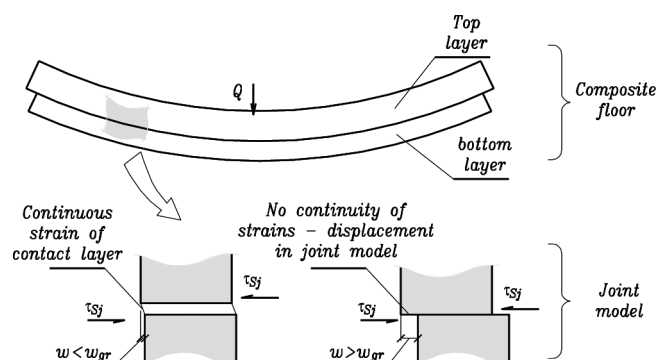

Fig. 1. Composite working model for two layers in reinforced concrete floors when the relative displacements of the layers (w) are smaller than the boundary value (w_{gr}) and when the displacements are larger than this value.

Rys. 1. Założenia dotyczące pracy zespolenia w żelbetowych płytach warstwowych poczynione na podstawie wyników badań doświadczalnych [1], w przypadku, gdy wzajemne przemieszczenia warstw (w) są mniejsze od wartości granicznej (w_{gr}) oraz gdy przemieszczenia warstw są większe od tej wartości

If the stiffness of the contact layer is small, and the displacement of the bottom layer is more than w_{gr}, the slippage is experienced of the bottom layer relative to the top layer, and the continuity of strains in the composite is not maintained (Fig. 1). In such situation, non-conservative kinetic friction forces are induced in the composite surface in the loading process. In the unloading process on the other hand, the static friction forces exist between the bottom and top layer. The issues were analysed in [2].

The subject of this work is a model of a continuous contact layer where continuous strains are produced under loading, (i.e. bottom layer displacements relative to the top layer are smaller than w_{gr}), and model of single degree of freedom of a composite floor is used.

The models defined below, together with the experimental investigations undertaken, sets a basis for developing a method of determining the state of the composite in

reinforced concrete floors based on energy dissipation in the composite. The stiffness of the composite determines the amount of energy to be dissipated.

The research on the composite concrete – concrete-type constructions was primarily focussed on investigating their load capacity. The impact on the composite load capacity was examined in particular for: the formation of the concrete layers' contact [3], concrete strength in the composite, and the percentage of the vertical reinforcement used in the composite surface [4], and the amount of the reinforced span reinforcement in the support [5]. It was also pointed out that the load capacity is also influenced by the stiffness of the composite of two concretes [6]. Proposals for calculating the composite load capacity depending on the joint geometry and the strength of the materials applied are presented notably in [7] and are envisaged by the majority of relevant standards [8].

The other group of the issues tackled by researchers was the impact of rheological phenomena on the static work of the composite elements being bent. Experimental studies were conducted, as well as theoretical ones, by taking into account different models of creep [9].

An analysis of the mechanical and physiochemical phenomena occurring at the contact of the composite elements should be distinguished as the third group of aspects pursued by the researchers [4], [10].

The literature concerning bridge structures indicates the possibility of investigating the variations in the dynamic properties of bridge structures as a consequence of the developing damages. However, the modal parameters must be changed constantly in this approach [11].

The review of the literature shows that no works have been carried out to-date examining losses of energy occurring within the composite of two concretes. No research methodology has been established, either, the purpose of which is to identify the state of the composite in the existing structures and to estimate, on such a basis, the transmissibility of forces by the composite in the ultimate limit state.

3. Models of the statically loaded contact layer and reinforced concrete composite floor

A band of a reinforced concrete composite floor is considered as working in one direction with b width loaded with the vertical force Q (Fig. 2). The load causes the non-dilatational strains of the contact layer (γ) observed as the displacement (w) of the bottom layer relative to the top layer. As a result of such displacement, the q reaction expressed with N/m occurs in the contact layer. In addition, the forces induced in the bottom and top layers, working as a result of bending, are a response to the Q load.
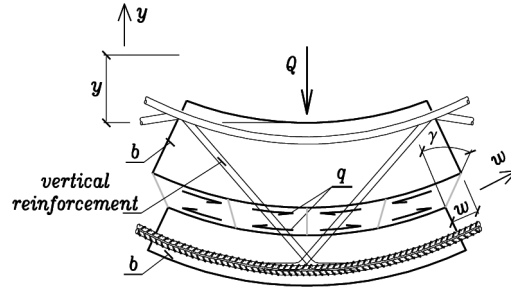
Fig. 2. Non-dilatational strains of the contact layer (γ) and relative displacement of the bottom and top layer (w).

Rys. 2. Odkształcenia postaciowe (γ) warstwy kontaktowej oraz wzajemne przemieszczenia warstwy dolnej względem górnej (w)

3.1. STIFFNESS OF THE MODEL OF CONTINUOUS CONTACT LAYER

A model of a continuous contact layer is represented by two serially connected elements (Fig 3a), i.e. a linear and elastic element and elastic frictional element. The linear and elastic element is characterised by the stiffness $k_{q,w,el}$ expressed in N/m^2 defined as a quotient of the q force by the corresponding elastic displacement $w_{q,el}$ (Fig. 3b)

$$(3.1) \qquad k_{q,w,el} = \frac{q}{w_{q,el}}.$$

The movement of the linear and elastic element in the static loading and unloading process is carried out in the straight line (Fig 3c).

The elastic and frictional element is modelling the non-conservative forces of internal friction and has a bilinear characteristic. The element, under the growing load, is characterised by linear stiffness $k_{q,w,fr-int}$ expressed with N/m^2 and is defined as

$$(3.2) \qquad k_{q,w,fr-int} = \frac{q}{w_{q,fr-int}},$$

where $w_{q,fr-int}$ is the displacement of the elastic and frictional element (Fig. 3b). Internal friction forces with the value q_{fr-int} (Fig. 3d) exist in the element during unloading. For this reason, the movement of the elastic and frictional element in the process of static unloading is represented by a vertical line in the configuration ($w_{q,fr-int}$, q). If the elastic and frictional element is loaded cyclically within the range of $-q_0 \div q_0$, then its movement takes place accordingly to a hysteresis loop (Fig. 3d).

With the growing load (q), the system (Fig. 3a) is characterised by linear substitute stiffness $k_{q,w,z}$ corresponding to two springs serially linked,

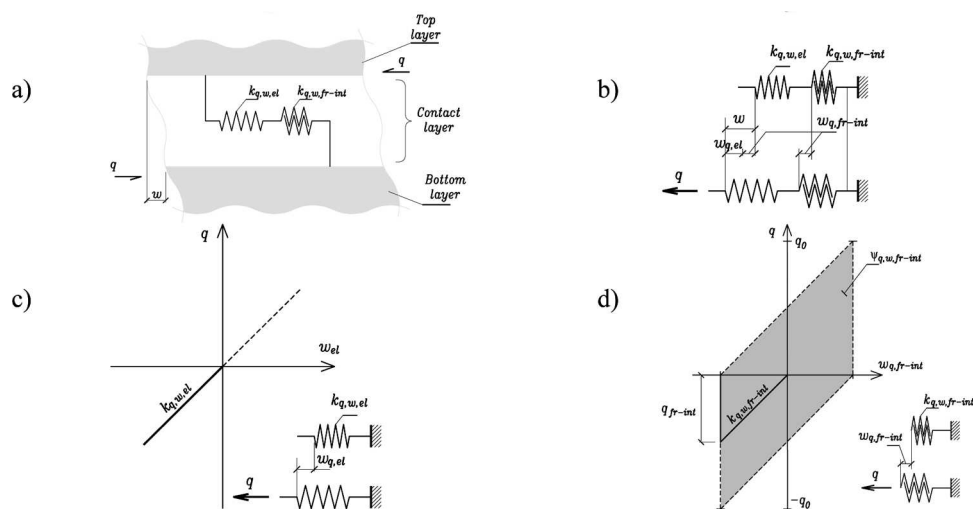$$(3.3) \qquad k_{q,w,z} = \frac{k_{q,w,el} \cdot k_{q,w,fr-int}}{k_{q,w,el} + k_{q,w,fr-int}}.$$

Fig. 3. Element of a model of continuous contact layer a) two serially connected stiffness representing: linear and elastic properties ($k_{q,w,el}$) and linear and frictional properties ($k_{q,w,fr-int}$), b) adopted designations of displacements, c) element modelling the elastic properties, d) hysteresis loop of the element modelling linear and frictional properties.

Rys. 3. Modelowanie ciągłej warstwy kontaktowej a) elementy modelujące: cechy liniowo – sprężyste ($k_{q,w,el}$) i sprężysto-tarciowe warstwy kontaktowej ($k_{q,w,fr-int}$), b) przyjęte oznaczenia przemieszczeń, c) charakterystyka elementu modelującego właściwości liniowo-sprężyste, d) pętla histerezy elementu modelującego właściwości sprężysto-tarciowe

and for unloading, it is characterised by the stiffness of $k_{q,w,el}$ (Fig 4a). The $k_{q,w,z}$ value, depending on the properties of concrete and on the formation of the composite in the tests [1] performed on slabs that are b=0.59 m wide, ranged between $0.5 \cdot 10^9$ N/m^2 to $140 \cdot 10^9$ N/m^2. On the other hand, composite stiffness determined in [6] for noticeable cracks is between 10 MPa to 170 MPa, and between 4 000 MPa to 54 000 MPa for the unnoticeable cracks. The author's experience shows that it is hard to determine $k_{q,w,z}$ where the stiffness of the composite is high, because small values of displacements (w), of around 10^{-3} mm, must be measured between the top and bottom layer.

The surface of the hysteresis loop of the single element modelling continuous contact layer, designated as $\psi_{q,w}$ (Fig 4a), corresponds to the energy dissipated by the elastic and frictional element in the cycle of full loading and unloading, and corresponds to

$$(3.4) \qquad \psi_{q,w} = 4q_{fr-int} \cdot w_{fr-int}.$$

The centre of the hysteresis loop is moved by the section 0 - 0' in relation to the point 0' where the loading of the system started and which represents the start of the system (w', q') (Fig 4a). The point 0 is considered the start of a new system of coordinates (w, q) where the model will be described further.
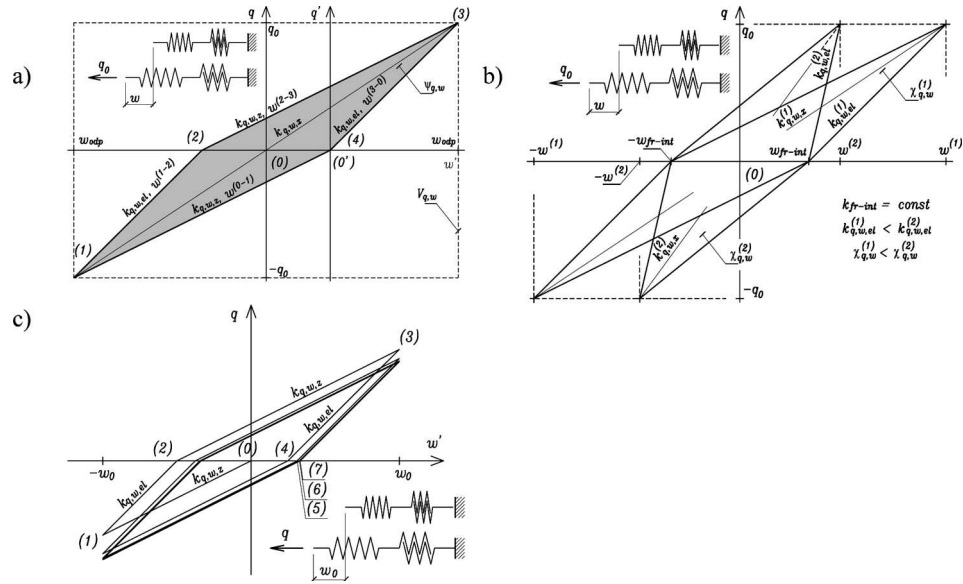
Fig. 4. Hysteresis loop of an element of the model of continuous contact layer a) loop structure with load capacity variations between $-q_0$, q_0, b) impact of variation in the stiffness $k_{q,w,el}$ on the energy dissipation coefficient, c) hysteresis loop structure with displacement forced within the range of $-w_0$, w_0.
Rys. 4. Pętla histerezy elementu modelu warstwy kontaktowej a) budowa pętli przy zmianie obciążenia w zakresie $-q_0$, q_0, b) wpływ zmiany sztywności $k_{q,w,el}$ na współczynnik dyssypacji energii elementu modelu warstwy kontaktowej ($\chi_{q,w}$), c) budowa pętli histerezy przy wymuszeniu przemieszczenia w zakresie $-w_0$, w_0

The loop from the figure (Fig 4a) can be inscribed into a rectangle with its sides having the length of $4q_{fr-int}$, $2w_{odp}$ and its area of

$$(3.5) \qquad V_{q,w} = 8q_{fr-int}w_{odp}.$$

A diagonal of the rectangle represents the resultant stiffness of the composite $k_{q,w,x}$ that can be determined experimentally based on the measurements of maximum "w" displacement of the bottom layer relative to the top layer. The value

$$(3.6) \qquad \chi_{q,w} = \frac{\psi_{q,w,fr-int}}{V_{q,w,fr-int}}$$

is referred to as an energy absorption coefficient in a composite. The coefficient in the composite model used assumes values between 0 and 0.5.

The following relationship can be expressed by taking into account the coefficient (3.5) and (3.2).

$$(3.7) \qquad \chi_{q,w} = \frac{w_{fr-int}}{2w_{odp}}$$

Taking into consideration (3.2), (3.7) and $w_0 = 2q_{fr-int} / k_{q,w,x}$, which results from the figure (Fig. 3d), the stiffness $k_{q,w,fr-int}$ is determined as dependent on the $k_{q,w,x}$ that can be determined experimentally ($k_{q,w,x}$ in tests is represented as $k_{q,w}$)

$$(3.8) \qquad k_{q,w,fr-int} = \frac{k_{q,w,x}}{4\chi_{q,w}}.$$

On the other hand, the following is determined according to the relationships (3.1), (3.2) and the condition $w_{el} = w_0 - w_{fr-int}$

$$(3.9) \qquad k_{q,w,el} = \frac{k_{q,w,x}}{1 - 2\chi_{q,w}}.$$

The following relationship is obtained by substituting (3.8) and (3.9) to (3.3)

$$(3.10) \qquad k_{q,w,z} = \frac{k_{q,w,x}}{1 + 2\chi_{q,w}}.$$

For the constant stiffness of $k_{q,w,fr-int}$, the coefficient $\chi_{q,w}$ assumes smaller values for smaller stiffness $k_{q,w,el}$ (Fig. 4b). If the $k_{q,w,fr-int}$ is growing without limits and $k_{q,w,el} = k_{q,w,z}$, then the coefficient $\chi_{q,w}$ assumes a near-zero value meaning that the model of the contact layer from the figure (Fig. 3a) does not dissipate energy. As demonstrated further, the situation corresponds to the contact layer with very small stiffness. On the other hand, in an inverse situation, where $\chi_{q,w}$ assumes a maximum value of 0.5, elastic displacements w_{el} do not occur because $k_{q,w,el}$ is rising without limits. As shown below, the situation corresponds to a composite with its high stiffness.

In the case of monolithic slabs, where no displacement occurs in the composite, the substitute stiffness $k_{q,w,z}$ can assume any value. Therefore, according to the relationship (3.3), both $k_{q,w,fr-int}$, $k_{q,w,el}$ as well as $k_{q,w,el}$, have any value, and $\chi_{q,w}$, according to the relationship between (3.8) to (3.10), is indefinite.

Note-worthy is the fact that, according to (3.2), (3.8) and (3.9), the force in the elastic and frictional element is

$$(3.11) \qquad q_{w,fr-int} = \frac{1}{2}k_{q,w,z}w_0\left(1 + 2\chi_{q,w}\right)$$

and it depends most of all on the displacement w_0 and on the substitute stiffness $k_{q,w,z}$. In addition, the force in this element, for the given displacement (w) in the composite, is higher in the elements characterised by the higher value $\chi_{q,w}$.

Finally, it is noted that if the model of the contact layer is loaded with a kinematic excitation, within the displacement range of $-w_0$, w_0, an unestabilised hysteresis loop is obtained. This means that the final point of the first hysteresis loop (point (4) – Fig. 4c) does not coincide with the final point of the second loop (point (5) – Fig. 4c), and this point, again, does not coincide with the final point of the third loop (point

(6) – Fig. 4c), and so on. However the distance between the final points of the next loops is decreasing so that the fourth loop can be considered as stabilised in the case analysed in (Fig. 4c). A stabilised loop is characterised by the same resultant stiffness $k_{q,w,x}$, by the same field $\psi_{q,w}$ and by the same coefficient $\chi_{q,w}$ as the loop produced when loading the model within the range of $-q_0$, q_0 with the same stiffness $k_{q,w,fr-int}$ and $k_{q,w,el}$.

3.2. A Model of a bent monolithic slab

A model of single degree of freedom of a bent monolithic slab is represented by two elements connected in parallel (Fig. 5a) the displacements of which are equal and designated as $y_{Q,m}$. Linear elasticity is represented by an element with the stiffness $k_{Q,m,el}$ expressed with N/m being a quotient of the force $Q_{m,el}$ that is acting vertically on such element, in Newtons, by the corresponding displacement $y_{Q,m}$ in meters (Fig. 5b)
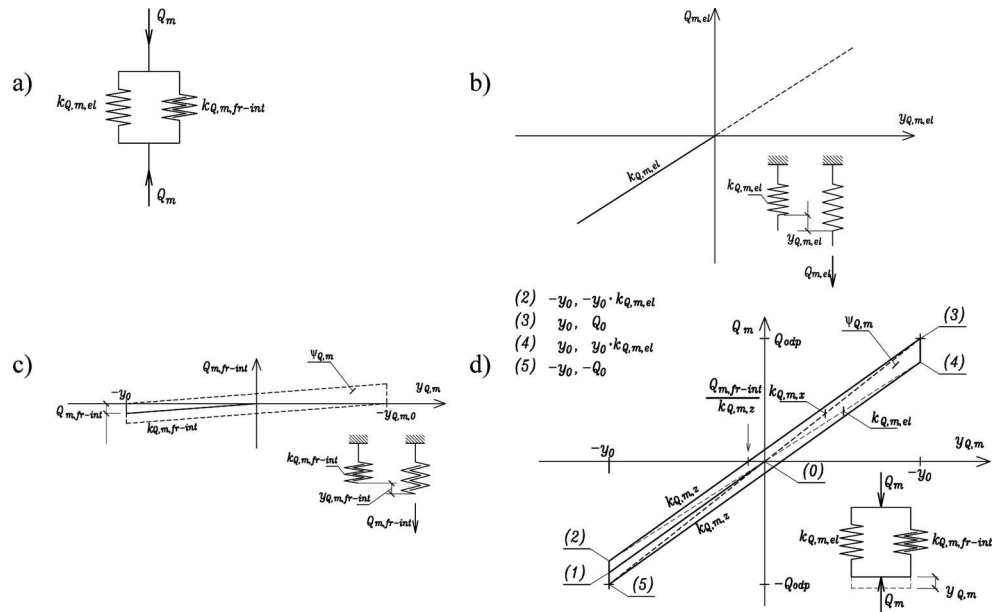

Fig. 5. Model of monolithic slab of single degree of freedom a) parallel bonding of the linear elastic element ($k_{Q,m,el}$) and elastic and frictional element ($k_{Q,m,fr-int}$), b) elastic element characteristic, c) elastic and frictional element characteristic, d) hysteresis loop of the model of monolithic slab for displacement excitation $- y_{Q,m,0}$, $y_{Q,m,0}$.
Rys. 5. Model płyty monolitycznej o jednym stopniu swobody a) połączenie równoległe elementów liniowo-sprężystego ($k_{Q,m,el}$) i sprężysto-tarciowego ($k_{Q,m,fr-int}$), b) charakterystyka elementu liniowo-sprężystego, c) charakterystyka elementu sprężysto-tarciowego, d) pętla histerezy modelu płyty monolitycznej w zakresie wymuszenia przemieszczeniem $-y_0$, y_0

$$(3.12) \qquad k_{Q,m,el} = \frac{Q_{m,el}}{y_{Q,m}}.$$

Internal friction in an element loaded statically which, in actual slabs, is generated mainly by the reinforcement working in the surrounding of vertical cracks, and is represented by an element with a bilinear characteristic described by the $k_{Q,m,fr-int}$ and the static friction force $Q_{m,fr-int}$ manifested when the element is unloaded (Fig. 5c). The stiffness of the elastic and frictional element is defined, accordingly, as a quotient of the relevant force to displacement

$$(3.13) \qquad k_{Q,m,fr-int} = \frac{Q_{m,fr-int}}{y_{Q,m}}.$$

With the rising load, the model is characterised by the substitute stiffness of $k_{Q,m,z}$ (Fig. 5d)

$$(3.14) \qquad k_{Q,m,z} = k_{Q,m,el} + k_{Q,m,fr-int}.$$

A precondition for the return movement during unloading, after reaching an extreme displacement, is to release the forces of internal friction. Therefore, in the unloading process in the extreme position – y_0 (Fig. 5d), a decrease of force in the system by the value $Q_{m,fr-int}$ is marked first. This can be interpreted as the apparent growth of the system stiffness (Fig. 5d). A permanent displacement occurs after unloading the system with the value of

$$(3.15) \qquad \frac{Q_{m,fr-int}}{k_{Q,m,z}}.$$

A hysteresis loop of the model of the slab of single degree of freedom is created, within the displacement range of $- y_{Q,m,0}$, $y_{Q,m,0}$, in the loading and unloading process with vertexes designated as (2)÷(5). Their coordinates ($y_{Q,m,i}$, $Q_{m,i}$, i=2...5) are provided in (Fig. 5d).

The area of the loop calculated according to the formula

$$(3.16) \qquad \psi_m = \sum_{i=2}^{5} Q_{m,i} \left(y_{Q,m,i+1} - y_{Q,m,i-1} \right)$$

is

$$(3.17) \qquad \psi_m = 4 y_{Q,m,0} \left(Q_0 - k_{Q,m,el} y_{Q,m,0} \right) .$$

By introducing the resultant stiffness $k_{Q,m,x}$ as a quotient

$$(3.18) \qquad k_{Q,m,x} = \frac{Q_{m,0}}{y_{Q,m,0}}$$

and considering that $Q_{m,fr-int} = (k_{Q,m,x} - k_{Q,m,el})y_{Q,m,0}$, the loop area can be expressed as

$$(3.19) \qquad \psi_{Q,m} = 4y_{Q,m,0}Q_{m,fr-int}$$

and the area of the rectangle into which the loop can be inscribed as

$$(3.20) \qquad V_{Q,m} = 4k_{Q,m,x}y_{Q,m,0}^2.$$

An energy dissipation coefficient defined by the quotient

$$(3.21) \qquad \chi_{Q,m} = \frac{\psi_{Q,m}}{V_{Q,m}}$$

after considering (3.19) and (3.20) is

$$(3.22) \qquad \chi_{Q,m} = \frac{k_{Q,m,fr-int}}{k_{Q,m,x}}$$

and can assume values between 0 and 0.5. By using the stiffness between (3.12) and (3.22), the specific stiffness can be expressed by the values $k_{Q,m,x}$ and $\chi_{Q,m}$ that can be determined in experimental studies (resultant stiffness $k_{Q,m,x}$ is equivalent to stiffness $k_{Q,m}$, determined experimentally at the point according to the hysteresis loop)

$$(3.23) \qquad \begin{aligned} k_{Q,m,fr-int} &= \chi_{Q,m}k_{Q,m,x}, \\ k_{Q,m,el} &= (1 - 2\chi_{Q,m})k_{Q,m,x}, \\ k_{Q,m,z} &= (1 - \chi_{Q,m})k_{Q,m,x}. \end{aligned}$$

If $k_{Q,m,fr-int}$ equals zero, then energy in monolithic slab is not dissipated, meaning that $\chi_{Q,m} = 0$, and $k_{Q,m,el} = k_{Q,m,x}$. In the situation where $\chi_{Q,m} = 0.5$ then $k_{Q,m,el}$ assumes a value equal to 0, $k_{Q,m,fr-int} = 0.5 \, k_{Q,m,x}$, and system deflection after unloading is $Q_{m,fr-int} / k_{Q,m,fr-int}$.

3.3. MODEL OF COMPOSITE FLOOR CONSIDERING THE STIFFNESS OF CONTACT LAYER

A model of an element of a continuous contact layer is described in the coordinates (w, q). A model of a monolithic slab of single degree of freedom is described in the coordinates (y, Q) (Fig. 2). In order to construct a model of a composite floor of single degree of freedom that takes into account a model of a contact layer, the description of the model of the contact layer should be changed from the coordinates (w, q_w) to the coordinates ($y_{Q,w}$, Q). Displacement $y_{Q,w}$ is the deflection of the slab model in the direction in which the force (Q) is acting. The displacement $y_{Q,w}$ is caused by displacement in the composite (w). In addition, the model of the contact layer should be combined adequately with the model of the monolithic slab.

The model of the monolithic slab and the model of the contact layer, under the rising load, behave linearly, and are characterised by the stiffness $k_{q,w,z}$ (3.3) and $k_{Q,m,z}$ (3.14). Hence, the relationship between the stiffness of the contact layer $k_{q,w,z}$ described in the coordinates (w, q_w) and the stiffness of this layer $k_{Q,w,z}$ described in the coordinates ($y_{Q,w}$, Q) can be examined with a linear and elastic numerical model FEM.

A numerical FEM model of the composite slab consists of three layers (Fig. 6a): a bottom layer that is h_d =0.07 m thick, a top layer that is h_g =0.11 m thick, and a contact layer that is h_w =0.003 m thick. The top and bottom layer is b = 0.59 m wide, whereas the width of the contact layer, designated as b_w, varied. The materials for all the layers is concrete with the elasticity modulus of E = 40 GPa and the Poisson coefficient of ν = 0.3.
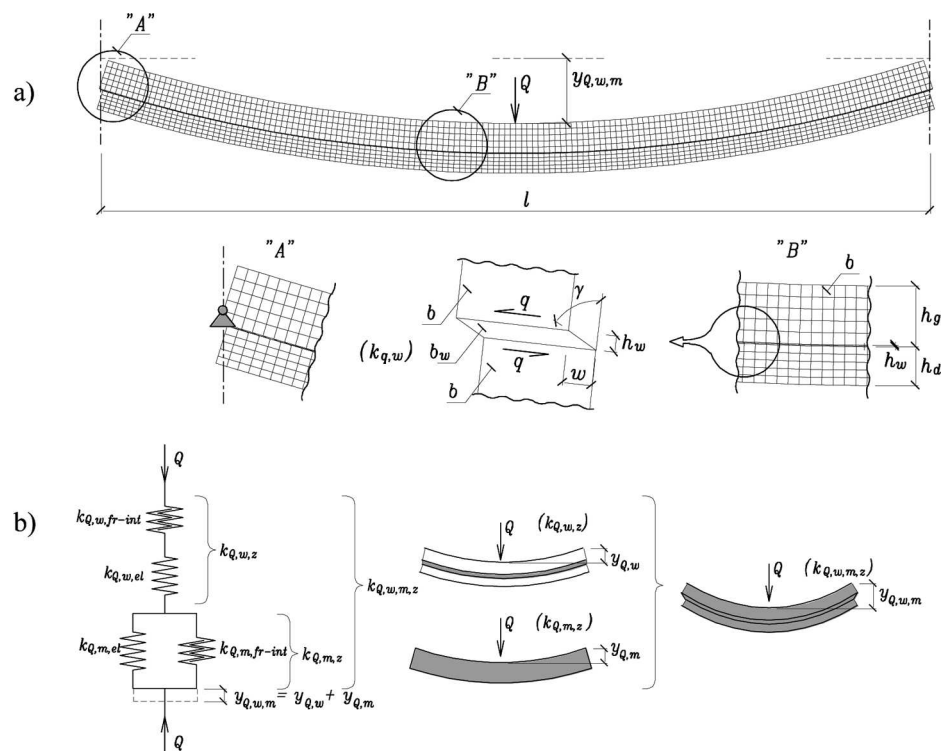

Fig. 6. Composite floor model a) FEM model, b) model of single degree of freedom built of linear and elastic and frictional elements.
Rys. 6. Modele płyty warstwowej a) model tarczowy (MES), b) model o jednym stopniu swobody zbudowany z elementów liniowo-sprężystych i sprężysto-tarciowych oraz interpretacja struktury modelu

The non-dilatational strain of the contact layer depends on the width of this contact layer and equals (Fig. 6a)

$$(3.24) \qquad \gamma = \frac{q_w}{G h_w},$$

and the displacement of the bottom layer relative to the top layer (w) is represented by the angle of non-dilatational strain (γ) multiplied by the height of the contact layer (h_w)

$$(3.25) \qquad w = \gamma \cdot h_w.$$

Taking into consideration the relationships (3.24) and (3.25) and the fact that $k_{q,w,z} = q_w/w$ occurs when the model is loaded, an expression for stiffness $k_{q,w,z}$ is obtained depending on the width of the contact layer of

$$(3.26) \qquad k_{q,w,z} = \frac{G}{h_w} b_w,$$

where as $G = E/(1+2\nu)$.

The displacement of the model of the composite slab of single degree of freedom impacted by both, the stiffness of the monolithic slab and the stiffness of the contact layer, was designated with $y_{Q,w,m,z}$. The inverse of the deflection $y_{Q,w,m,z}$ multiplied by the loading force Q represents the substitute stiffness of the composite slab

$$(3.27) \qquad k_{Q,w,m,z} = \frac{Q}{y_{Q,w,m,z}}.$$

The FEM model calculations were performed for a freely supported floor loaded with the concentrated force Q in the middle of the slab span (item A – Fig 6a). The width b_w in the calculations was changed starting from 0.59 m, which corresponded to the stiffness of $k_{q,w,z} = 4.92 \cdot 10^{12}$ N/m and to the monolithic slab's working conditions, to 10^{-11} m, which corresponded to the stiffness of $k_{q,w,z} = 86.9$ N/m. The stiffness of the composite slab $k_{Q,w,m,z}$ determined according to (3.27) is provided in Table 1. The deflection produced by the contact layer existing in the slab with the stiffness of $k_{Q,w,z}$ is calculated from the following relationship

$$(3.28) \qquad y_{Q,w,z} = y_{Q,m,z} - y_{Q,w,m,z}$$

where $y_{Q,m,z}$ is the monolithic slab deflection, i.e. the deflection of the model discussed above by assuming $b_w = b$ determined from the following relationship

$$(3.29) \qquad k_{Q,m,z} = \frac{Q}{y_{Q,m,z}}.$$

Results of numeric (FEM) calculation.
Wyniki obliczeń numerycznych (MES) modelu płyty warstwowej

b_w [m]	$k_{q,w,z}$ [N/m²]	$k_{Q,w,m,z}$ [N/m]	$k_{Q,w,z}$ [N/m]	b_w [m]	$k_{q,w,z}$ [N/m²]	$k_{Q,w,m,z}$ [N/m]	$k_{Q,w,z}$ [N/m]
0,59	$4,92 \cdot 10^{12}$	$2,03 \cdot 10^7$	$3,76 \cdot 10^9$	10^{-6}	$8,69 \cdot 10^6$	$7,87 \cdot 10^6$	$1,29 \cdot 10^7$
10^{-1}	$8,33 \cdot 10^{11}$	$2,02 \cdot 10^7$	$5,00 \cdot 10^9$	10^{-7}	$8,69 \cdot 10^5$	$7,19 \cdot 10^6$	$1,11 \cdot 10^7$
10^{-2}	$8,33 \cdot 10^{10}$	$1,98 \cdot 10^7$	$9,09 \cdot 10^8$	10^{-8}	$8,69 \cdot 10^4$	$6,91 \cdot 10^6$	$1,05 \cdot 10^7$
10^{-3}	$8,33 \cdot 10^{09}$	$1,74 \cdot 10^7$	$1,22 \cdot 10^8$	10^{-9}	$8,69 \cdot 10^3$	$6,87 \cdot 10^6$	$1,04 \cdot 10^7$
10^{-4}	$8,33 \cdot 10^{08}$	$1,12 \cdot 10^7$	$2,49 \cdot 10^7$	10^{-10}	$8,69 \cdot 10^2$	$6,87 \cdot 10^6$	$1,04 \cdot 10^7$
10^{-5}	$8,33 \cdot 10^{07}$	$8,49 \cdot 10^6$	$1,46 \cdot 10^7$	10^{-11}	$86,9$	$6,87 \cdot 10^6$	$1,04 \cdot 10^7$

The substitute stiffness of the composite in the direction where the force Q is acting is defined as

$$(3.30) \qquad k_{Q,w,z} = \frac{Q}{y_{Q,m,z}}$$

and, considering the relationships (3.28) and (3.30), is expressed by means of the substitute stiffness of the monolithic and composite slab

$$(3.31) \qquad k_{Q,w,z} = \frac{k_{Q,w,z} k_{Q,w,m,z}}{k_{Q,w,z} - k_{Q,w,m,z}}.$$

The relationship between $k_{q,w,z}$, described in the coordinates (w, q_w), and the substitute stiffness of $k_{Q,w,z}$, described in the coordinates $(y_{Q,w}, Q)$ and determined with a numerical model (Fig. 6a), is provided in the figure (Fig. 7).
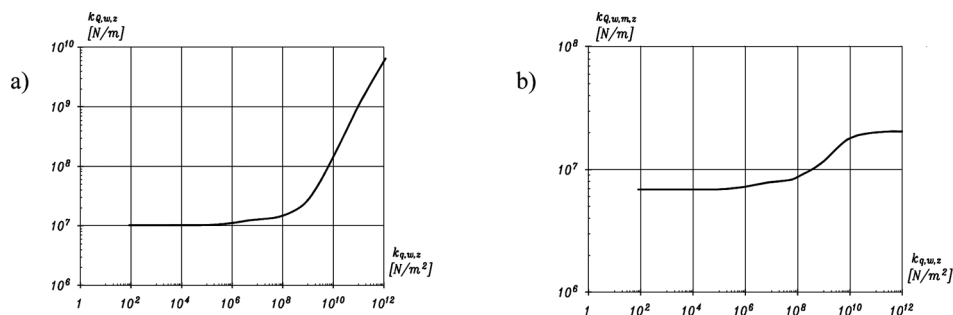

Fig. 7. Relationships between stiffness determined in FEM model a) $k_{Q,w,z}$ ($k_{q,w,z}$) b) $k_{Q,w,m,z}$ ($k_{q,w,z}$).
Rys. 7. Zależności między sztywnościami wyznaczonymi pod narastającym obciążeniem w modelu tarczowym (MES) a) $k_{Q,w,z} - k_{q,w,z}$ b) $k_{Q,w,m,z} - k_{Q,w,z}$

The relationship (3.28) means that model for the composite slab is the serial combination of the model of the contact layer and the model of the monolithic slab (Fig. 6b).

A hysteresis loop of the model of the composite floor is developed by assuming that the structure of the model of the composite slab is the same also during unloading, when non-linear effects appear defined in the previous section. Two such loops are provided in (Fig. 8) for $\chi_{q,w} < 0.5$ and $\chi_{q,wt} = 0.5$. An area of the hysteresis loop of the model of composite slab $\psi_{Q,m}$ is larger for the slabs characterised by a higher coefficient $\chi_{q,w}$. While defining the coefficient $\chi_{q,w}$ for the model of the composite slab one can note that, the same as in the models of the composite and of the monolithic slab, as the quotient
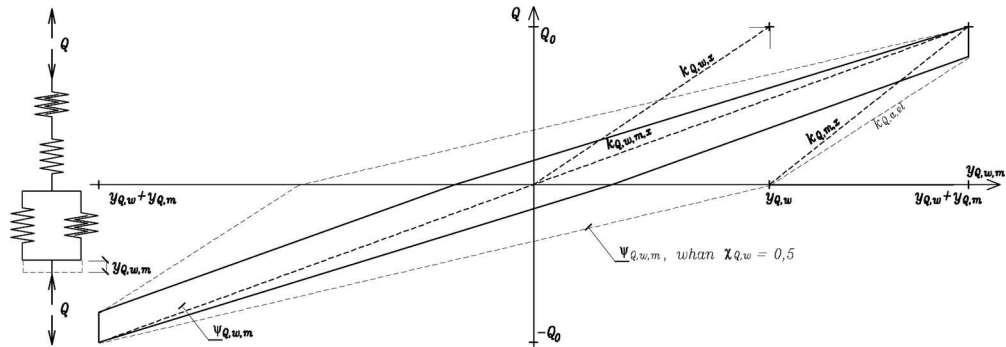

Fig. 8. Shape of the hysteresis loop of the slab model according to energy dissipation in the composite. The continuous line corresponds to $\chi_{q,w} < 0.5$ and the intermittent line to $\chi_{q,w} = 0.5$
Rys. 8. Kształt pętli histerezy modelu płyty warstwowej o jednym stopniu swobody w zależności od wartości współczynnika dyssypacji energii w zespoleniu ($\chi_{Q,w}$); linia ciągła odpowiada $\chi_{Q,w} < 0.5$ a linia przerywana odpowiada $\chi_{Q,w} = 0.5$

$$(3.32) \qquad \chi_{Q,w,m} = \frac{\psi_{Q,w,m}}{V_{Q,w,m}}$$

while decreasing the stiffness of the contact layer, the value is falling. This results directly from the growing deflection caused by the decreased stiffness of the composite ($y_{Q,w}$ – Fig. 8).

4. MODEL OF A DYNAMICALLY LOADED COMPOSITE SLAB

Internal friction in the structures loaded dynamically demonstrates itself as viscous forces [12] the value of which is proportional to the rate of deformation. Such forces are performing work and cause energy to dissipate. The continuous strains of the contact layer are analysed in the model presented. For this reason, no damping is investigated related to the kinematic friction of the bottom layer relative to the top layer.

It analogously assumed as for the model from the figure (Fig. 6b) that the element of a model of continuous contact layer is represented by the serial connection of the element with the stiffness $k_{q,w}$ (3.3) and of the energy dissipating element described by the Newton law. The following relationship is a physical relationship describing an element of the model of the continuous contact layer in the coordinates (w, q_w)

$$(4.1) \qquad \dot{w} = \frac{\dot{q}}{k_{q,w}} + \frac{q}{c_{q,w}},$$

where $c_{q,w}$ is a damping coefficient expressed in kg/(m·s), and $\dot{w}$ is the rate of displacement of the top layer relative to the bottom layer (Fig. 9a). The relationship (4.1) is the same as the equation describing a Maxwell body [13]. The influence of the continuous contact layer on the model of single degree of freedom in the system of coordinates ($y_{Q,w}$, S_w), where S_w is designated as the internal force (Fig. 9b), analogous to (4.1) is described as
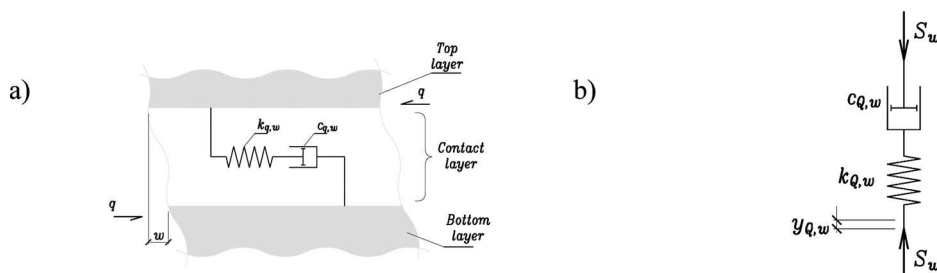

Fig. 9. Contact layer modelling a) Maxwell body as an element of a model of continuous contact layer, b) model of single degree of freedom representing contact layer.
Rys. 9. Modelowanie warstwy kontaktowej a) ciało Maxwella jako model ciągłej warstwy kontaktowej, b) element modelujący wpływ warstwy kontaktowej w modelu płyty warstwowej o jednym stopniu swobody

$$(4.2) \qquad \dot{y}_{Q,w} = \frac{\dot{S}_w}{k_{Q,w}} + \frac{S_w}{c_{Q,w}}.$$

The damping coefficient $c_{Q,w}$ is expressed in kg/s.

An element with stiffness $k_{Q,m}$ connected parallel with the energy dissipating element is the model of the monolithic slab of single degree of freedom loaded dynamically,

analogously to the model from (Fig. 5a). By assuming, as above, that the energy dissipating element describes the Newton law with the damping coefficient $c_{Q,m}$, the internal force S_m equals

(4.3)
$$S_m = k_{Q,m} \cdot y_{Q,m} + c_{Q,m} \cdot \dot{y}_{Q,m}.$$

The above equation is the same as the relationship describing a Kelvin – Voigt body [13].

4.3. MODEL OF COMPOSITE FLOOR CONSIDERING THE STIFFNESS OF THE CONTACT LAYER

A model of the slab of single degree of freedom subjected to a dynamic load is represented by the parallel connection of the model of the contact layer and the model of the monolithic slab. This derives from the assumption that the displacement of the composite slab in the direction of the acting load Q ($y_{Q,w,m}$) is a sum of the displacements of the model of the monolithic slab ($y_{Q,m}$) and of the displacement ($y_{Q,w}$), that are resulting from the occurrence of the contact layer. What is new, as compared to the existing elaborations discussing the dissipation of energy during vibrations (for example [14], [15]), is that a physical interpretation is assigned to the particular elements of the model from the figure (Fig. 11a), and that continuity is ensured between the static and dynamic model of the composite slab. A Maxwell or Kelvin-Voigt body is considered in the relevant literature [14], [15].
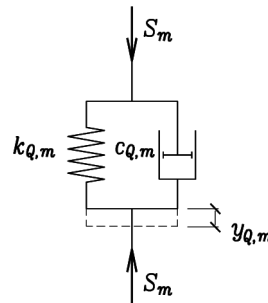

Fig. 10. A Kelvin-Voigt body as a model of the monolithic floor.
Rys. 10. Element o strukturze ciała Kelvina-Voigta jako model płyty monolitycznej

A differential equation is obtained for the displacement of the model of the composite slab ($y_{Q,w,m}$) by multiplying the equation (4.2) by $k_{Q,m}$ and the equation (4.3) by $c_{Q,m}$, and then by adding the multiplied equations, and by considering that $y_{Q,w,m} = y_{Q,w} + y_{Q,m}$. The following relationship is formulated by differentiating further the equation produced and then by multiplying by the quotient $c_{Q,w}/k_{Q,m}$

(4.4) $$S + \dot{S}\underbrace{\left(\frac{c_{Q,m}}{k_{Q,m}} + \frac{c_{Q,w}}{k_{Q,w}} + \frac{c_{Q,w}}{k_{Q,m}}\right)}_{a} + \ddot{S}\underbrace{\frac{c_{Q,m}}{k_{Q,w}}\frac{c_{Q,w}}{k_{Q,m}}}_{b} = \dot{y}_{Q,w,m} \cdot \underbrace{c_{Q,w}}_{c} + \ddot{y}_{Q,w,m}\underbrace{\frac{c_{Q,m} \cdot c_{Q,w}}{k_{Q,m}}}_{d}.$$

The relationship describes the response S to displacement $y_{Q,w,m}$ of the model characterised by the velocity $\dot{y}_{Q,w,m}$ and acceleration $\ddot{y}_{Q,w,m}$. The structure of the equation corresponds to a Bürgers body [16].
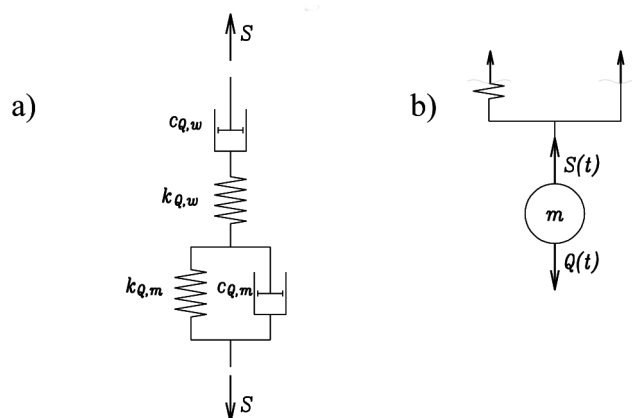

Fig. 11. The model of a dynamically loaded composite floor a) a Bürgers body where S is internal force, b) a model of the floor with weight attached and load with a variable force S.
Rys. 11. Model płyty warstwowej o jednym stopniu swobody obciążony dynamicznie a) element o strukturze ciała Bürgersa, w którym występuje siła wewnętrzna S, b) model płyty warstwowej o jednym stopniu swobody z dołączoną masą i obciążony zmienną siłą Q

By applying mass and an external load Q(t) variable in time (Fig. 11b) to the model from the figure (Fig. 11a), and then by assuming that the force of inertia of the mass (m) moving with the acceleration $\ddot{y}_{Q,w,m}$ has the opposite sense to the loading force (Q(t)), and the internal force (S) has the opposite sense to the load (Q), then the equation of the element with the mass (m) is as follows

$$(4.5) \qquad m \cdot \ddot{y}_{Q,w,m} = Q(t) - S(t).$$

The following is obtained by substituting the expression (4.5) to (4.4) and by ordering it

$$(4.6) \qquad Q + a\dot{Q} + \ddot{Q}b = c\dot{y}_{Q,w,m} + (d + m)\ddot{y}_{Q,w,m} + may_{Q,w,m} + mb\dddot{y}_{Q,w,m},$$

where a, b, c is according to (4.4).

The author conducts the experimental verification of the analyses performed by examining the free vibrations of composite slabs during which the external load Q(t) equals zero and the initial conditions exist

$$(4.7) \qquad y_{Q,w,m}(0) = -y_0, \; \dot{y}_{Q,w,m}(0) = \ddot{y}_{Q,w,m}(0) = y_{Q,w,m}(0) = 0.$$

After considering the above conditions and after differentiating once the equation (4.6), the final equation was obtained of free slab vibrations

(4.8)
$$m\frac{c_{Q,m}}{k_{Q,w}}\dddot{y}_{Q,w,m} + m\left(\frac{c_{Q,m}}{c_{Q,w}} + \frac{k_{Q,m}}{k_{Q,w}} + 1\right)\ddot{y}_{Q,w,m} + \left(c_{Q,m} + m\frac{k_{Q,m}}{c_{Q,w}}\right)\dot{y}_{Q,w,m} + k_{Q,m}y_{Q,w,m} = -k_m y_0.$$

Note that if stiffness in the composite $k_{Q,w}$ and the damping coefficient $c_{Q,w}$ in the composite grow inorganically, then the equation (4.8) comes down to the commonly known equation describing vibrations with viscous damping

(4.9)
$$m\ddot{y}_{Q,m} + c_{Q,m}\dot{y}_{Q,m} + k_{Q,m}y_{Q,m} = -k_{Q,m}y_0.$$

4.4. Free damped vibrations of the model of the composite slab

It is assumed that free vibrations are induced by releasing suddenly the force loading the model which can be achieved physically by removing a temporary support installed at the centre of the span of the slab, where force – Q_0 was induced statically. The following initial deflection value y_0 was assumed in the slab state equation (4.8) before removing the support

(4.10)
$$y_0 = \frac{Q_0}{k_{Q,w,m}}$$

and the value is substituted in the equation (4.8), leading to the following relationship

(4.11)
$$m\frac{c_{Q,m}}{k_{Q,w}}\dddot{y}_{Q,w,m} + m\left(\frac{c_{Q,m}}{c_{Q,w}} + \frac{k_{Q,m}}{k_{Q,w}} + 1\right)\ddot{y}_{Q,w,m} + \left(c_{Q,m} + m\frac{k_{Q,m}}{c_{Q,w}}\right)\dot{y}_{Q,w,m} + $$
$$+ k_{Q,m}y_{Q,w,m} = -k_{Q,m}\frac{Q_0}{k_{Q,w,m}}.$$

The following is obtained by introducing a new variable

(4.12)
$$\xi = y_{Q,w,m} - \frac{Q_0}{k_{Q,w,m}}$$

and by substituting the variable to the equation (4.11)

(4.13)
$$m\frac{c_{Q,m}}{k_{Q,w}}\dddot{\xi} + m\left(\frac{c_{Q,m}}{c_{Q,w}} + \frac{k_{Q,m}}{k_{Q,w}} + 1\right)\ddot{\xi} + \left(c_{Q,m} + m\frac{k_{Q,m}}{c_{Q,w}}\right)\dot{\xi} + k_{Q,m}\xi = 0.$$

The above equation can be recorded as follows

(4.14)
$$a_1 \cdot \dddot{\xi} + b_1 \cdot \ddot{\xi} + c_1 \cdot \dot{\xi} + d_1\xi = 0,$$

and its solution is searched as an exponential function [17]

(4.15) $\xi(t) = e^{rt}$.

A characteristic equation is obtained by substituting an exponential function and its derivatives

(4.16) $a_1 \cdot r^3 + b_1 \cdot r^2 + c_1 \cdot r + d_1 = 0$,

the solution of which are the three elements r_1, r_2, r_3. If one element is real and two composite ones are complex, then the system vibrates. It can be thus assumed that

(4.17) $r_1 = -\alpha, \quad r_2 = -n_{w,m} + \omega_{w,m}i, \quad r_2 = -n_{w,m} - \omega_{w,m}i$.

The three functions are the particular integrals of the equation

(4.18) $\xi_1(t) = e^{-\alpha t}, \quad \xi_2(t) = e^{(-n_{w,m}+\omega_{w,m}i)t}, \quad \xi_3(t) = e^{(-n_{w,m}-\omega_{w,m}i)t}$.

The further transformations were conducted using Euler's equation

(4.19)
$$\begin{aligned}\xi_2(t) &= e^{-n_{w,m}t}\left(\cos\omega_{w,m}t + i\sin\omega_{w,m}t\right)\\ \xi_3(t) &= e^{-n_{w,m}t}\left(\cos\omega_{w,m}t - i\sin\omega_{w,m}t\right)\end{aligned} \quad ,(4.19)$$

and in order to rid of the imaginary unit "i", new functions were introduced as combinations of the two above functions

(4.20)
$$\begin{cases} \bar{\xi}_2 = \dfrac{\xi_2 + \xi_3}{2} = e^{-n_{w,m}t}\cos(\omega_{w,m}t) \\[2mm] \bar{\xi}_3 = \dfrac{\xi_2 - \xi_3}{2i} = e^{-n_{w,m}t}\sin(\omega_{w,m}t) \end{cases}.$$

The total integral of the equation (4.13) is the linear combination of the three above functions

(4.21) $\xi(t) = C_1 e^{-\alpha t} + e^{-nt}\left(C_2 \cos(\omega t) + C_3 \sin(\omega t)\right)$

and the general solution of the output equation (4.11) has the form of

(4.22) $y_{Q,w,m}(t) = \dfrac{Q_0}{k_{Q,w}} + C_1 e^{-\alpha t} + e^{-nt}\left(C_2 \cos(\omega t) + C_3 \sin(\omega t)\right)$.

It is assumed according to the initial conditions (4.7) that in the initial moment of t = 0 the support is removed suddenly, meaning that the force Q_0 directed upwards is abruptly applied to the slab. The force is represented by the initial deflection y_0 multiplied by the stiffness $k_{Q,w}$

(4.23) $Q_0 = y_0 \cdot k_{Q,w}$.

The constants of integration are determined from the initial conditions

$$(4.24) \qquad y_{Q,w,m}(0) = \frac{Q_0}{k_{Q,w}}, \quad \dot{y}(0) = 0, \quad \ddot{y}(0) = 0.$$

The ultimate solution of the equation (4.11) is as follows

$$(4.25) \qquad y_{Q,w,m}(t) = \frac{Q_0}{k_{Q,w}} + C_1 e^{-\alpha t} + A_0 e^{-n_{w,m}t} \sin(\omega_{w,m}t + \phi)$$

where

$$(4.26) \qquad tg\phi = \frac{\alpha \omega_{w,m}(\alpha - 2n_{w,m})}{n_{w,m}\alpha^2 + \alpha \omega_{w,m}^2 - n_{w,m}^2 \alpha},$$

$$(4.27) \qquad A_0 = Q_0 \frac{\sqrt{\alpha^2 (\alpha - 2n_{w,m})^2 + \left(\omega_{w,m}^2 + n_{w,m}^2\right)^2}}{k_{Q,a,z}\left(\omega_{w,m}^2 + n_{w,m}^2 + \alpha^2 - 2n_{w,m}\alpha\right)}.$$

The figure (Fig. 12) presents the solution (4.25) graphically. One of the parameters describing energy dissipation when vibrations are performed by the model composite slab is the damping coefficient being the quotient of
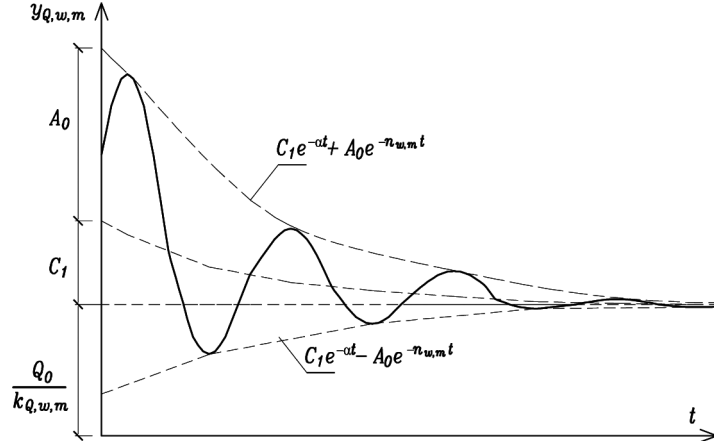
Fig. 12. Graphical representation of the equation solution (4.25).
Rys. 12. Graficzna interpretacja rozwiązania równania (4.25)

$$(4.28) \qquad \zeta_{w,m} = \frac{n_{w,m}}{\omega_{w,m}}$$

where

$$(4.29) \qquad \omega_{w,m} = \sqrt{\frac{k_{Q,w,m,z}}{m}}$$

is referred to as the natural angular frequency of the model of composite slab damping vibrations with the stiffness of $k_{Q,w,m}$ and the modal mass of m.

Variations to the critical damping ratio $\zeta_{w,m}$, corresponding to the first form of the model of composite slab free vibrations according to the composite stiffness $k_{Q,w}$, is examined. The model of the slab examined is presented in figure (Fig. 6a) where the stiffness of the monolithic concrete floor at the point $k_{Q,m} = 2.03 \cdot 10^7$ N/m, and the modal mass as for the slab freely supported performing free vibrations corresponding to the first form with the assumed volume mass of $\rho = 24.5$ kN/m^3, is m = $17/35 \cdot l \cdot b \cdot (h_g + h_d) \rho = 379$ kg.

The damping coefficient $c_{Q,m}$ corresponding to the monolithic slab is assumed constant, is equal to

$$(4.30) \qquad c_{Q,m} = 2\zeta_m \sqrt{k_{Q,m,w} m},$$

where ζ_m is the monolithic slab critical damping coefficient with its value equal to 0.015.

The damping coefficient $c_{Q,w}$ corresponding to viscous damping, that is modelling damping in the composite, is dependent linearly on the stiffness $k_{Q,w}$ and is expressed with the following relationship

$$(4.31) \qquad c_{Q,w} = \frac{k_{Q,w}}{d},$$

where d is a constant changed in the calculations from 3 to 50.

It is justified to assume the relationship (4.31) in the remark made in chapter 3, where it is noted that force in the element modelling energy dissipation with constant displacement is dependent linearly on the substitute stiffness in the composite (3.11).

The component stiffness $k_{Q,w}$ in the calculations performed is changed from $1 \cdot 10^6$ N/m to $1 \cdot 10^9$ N/m. This corresponds to the stiffness of the composite slab $k_{Q,w,m}$ determined with the relationship (3.31) changing between $0.105 \cdot 10^9$ N/m to $2.00 \cdot 10^9$ N/m. Physically, the stiffness $k_{Q,w,m}$ can change from $0.585 \cdot 10^9$ N/m, which corresponds to the stiffness of two layers working independently to $2.03 \cdot 10^9$ N/m, which corresponds to the stiffness of the monolithic slab at point ($k_{Q,m}$).

The figure (Fig. 13a) presents a variation in the critical damping ratio $\zeta_{w,m}$ according to stiffness $k_{Q,w}$ and according to stiffness of the composite floor at the point $k_{Q,w,m}$ for the d parameter values of 3, 10, 20, 30, 50. In all the cases, the value $\zeta_{w,m}$ is approaching 0.015, along with the increased stiffness of the $k_{Q,w,m}$ (i.e. increased component stiffness of the composite floor $k_{Q,w}$), reaching this value in the situation

where the stiffness of the composite floor of $k_{Q,w,m,z}$ reaches the stiffness of the monolithic slab of $k_{Q,m} = 2.03 \cdot 10^9$ N/m. By omitting the small ranges of stiffness for d = 3 and 10, the growth of the critical damping fraction is observed along with the declining stiffness of the slab of $k_{Q,w,m}$. This means that the slabs with small stiffness of the contact layer will be characterised by greater value of the damping parameter $\zeta_{w,m}$. This conclusion is of basic importance for the experimental investigations held currently and is of a huge practical importance. As presented in the introduction, the destruction of slabs with small composite stiffness is accompanied by the slippage of the bottom layer relative to the top layer [1].
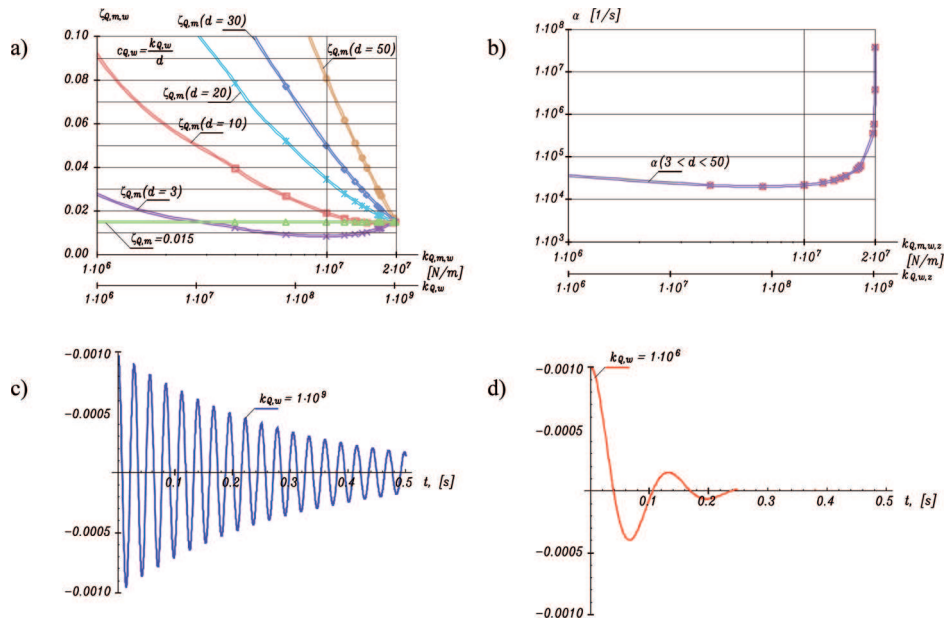

Fig. 13. Results of calculations for the composite floor model a) critical damping factor $\zeta_{m,w}$ as the function of the composite slab stiffness $k_{Q,w,m}$ and stiffness $k_{Q,w}$. The damping factor $c_{Q,w} = k_{Q,w}/d$ (d = 3, 10, 20, 30, 50) and damping ratio of monolithic slab $\zeta_m = 0.015$, b) the values of the exponent α, c), d) the fading of model vibrations by assuming: $k_{Q,m} = 2 \cdot 10^7$ N/m, $c_{Q,m}$ according to (4.30) by assuming $\zeta_m = 0.015$, $c_{Q,w} = k_{Q,w}/30$, m=379 kg and $k_{Q,w} = 1 \cdot 10^9$ N/m (Fig. c) and $k_{Q,w} = 1 \cdot 10^6$ N/m (Fig. d).
Rys. 13. Wyniki obliczeń modelu płyty warstwowej o jednym stopniu swobody a) ułamek tłumienia krytycznego płyty warstwowej ($\zeta_{m,w}$) jako funkcja sztywności płyty warstwowej $k_{Q,w,m}$ i sztywności opisującej wpływ warstwy kontaktowej $k_{Q,w}$; współczynnik tłumienia $c_{Q,w} = k_{Q,w,z}/d$ (d = 3, 10, 20, 30, 50) przy przyjęciu ułamka tłumienia krytycznego płyty monolitycznej $\zeta_m = 0,015$, b) wartości wykładnika α, c) zanikanie drgań modelu przy przyjęciu: $k_{Q,m} = 20 \cdot 10^6$ N/m, $c_{Q,m}$ według (4.30) przy założeniu $\zeta_m = 0,015$, $c_{Q,w} = k_{Q,w,z}/30$, m=379 kg oraz $k_{Q,w} = 1 \cdot 10^9$ N/m, d) jak (c) dla $k_{Q,w} = 1 \cdot 10^6$ N/m

A variation of the value α according to the stiffness of the slab $k_{Q,w,m}$ is presented in Fig. 13b. The values of this parameter are by several grades higher than the value $n_{w,m}$, meaning that it is irrelevant for the conducted analyses of fading of free vibrations.

Fig. 13c presents the curves of the damped vibrations obtained from the solution of the equation (4.13) for the high stiffness of the composite $k_{Q,w} = 1 \cdot 10^9$ N/m, and (Fig. 13d) for the small stiffness of the composite $k_{Q,w} = 1 \cdot 10^6$ N/m. The curves show huge differences both in the damping of the vibrations occurring according to the composite stiffness, and in the frequency of vibrations. The author obtains such curves during the experimental works conducted with the actual composite floors.

5. Summary

It was assumed that the composite reinforced concrete floor consists of the bottom layer, top layer and contact layer. A model of single degree of freedom of this floor was defined. It was assumed that elastic strains and inelastic strains existed in the elements of the model.

Studies into the model revealed that a hysteresis loop was created in the process of static loading and unloading allowing to determine the coefficient of energy dissipation for a static kinematic excitation. Model with low composite stiffness exhibits smaller values of such coefficient.

The defined model assumes that, during vibrations, the inelastic forces of internal friction in the composite and in the concrete of the bottom layer and of top layer are manifested as viscous friction. It is demonstrated that the vibrations of the model of the composite slabs characterised by low composite stiffness are damped stronger than the vibrations of the slabs with a stiff contact layer. Moreover, the lower stiffness of the element modelling the contact layer corresponds to the smaller frequencies of the model of free vibrations.

The above findings, concerning the dissipation of energy while loading a slab statically and dynamically, are of a great practical importance. This is due to the fact that, after being verified practically, they allow to determine the stiffness of the composite of two concretes in reinforced concrete composite floors. The investigations [1] revealed that the slabs with low composite stiffness reach a boundary value of displacement of w_{gr} under a lower load and a loss in their load capacity is accompanied by delamination.

The outcomes of the carried out theoretical analyses set one of the basis for the experimental investigations pursued at present into the dissipation of energy in the reinforced concrete floors subjected to kinematic, static, and dynamic excitations.

6. Acknowledgements

REFERENCES

1. K. GROMYSZ, *Testing stiffness of contact layer in composite concrete slabs* [in Polish]. The 56th Scientific Conference of the Civil and Environmental Engineering of the Polish Academy of Sciences and of the Committee of Science of the PZITB. Kielce – Krynica 19–24 September 2010, pages 529-537.

2. K. GROMYSZ, *Hysteresis loop of model of concrete composite slab* [in Polish]. Polish Academy of Sciences. Scientific and Research Problems of Construction Białystok University of Technology Editions, **6**, pages 187-194, Białystok 2008.

3. T. KAMADA, V.C. LI, *The effect of surface preparation on the fracture behavior of ECC/concrete repair system*, Cement and Concrete Composites, 22, 423-431, 2000.

4. A. HALICKA, *Shear bond test for analysis of composite concrete structures*, Proccedings 5 th International Conference AMCM 2005 "Analytical models and new concepts in concrete and masonry structures", Gliwice – Ustroń 2005, p. 53-54.

5. W. STAROSOLSKI, K. GROMYSZ, *Composite slab floors. Force distribution between contact surface and main bars anchored in ring beam* [in Polish], The VIIth Scientific Conference on Composite Structures, pages 133-143, Zielona Góra June 2005.

6. A. HALICKA, *A study of the stress – strain state in the interface and support zones of composite structures with shrinking and expansive concretes* [in Polish], Lublin University of Technology Editions, Lublin 2007.

7. K. GROMYSZ, *Combined floors*. Normative calculations guidecurves and capacity of actual structures. 5-th international conference AMCM Analytical Models and New Concepts in Concrete and Masonry Structures, Gliwice-Ustroń June 12-14 2005, p. 51-52.

8. Eurocode 2: Design of Concrete Structures – Part 1-1: General rules and rules for buildings. EN 1992-1-1:2004. European Committee for Standardization., Brussels 2004.

9. K. FURTAK, *Composite bridges* [in Polish], PWN, Warszawa – Kraków 1999.

10. K. GROMYSZ, *Calculation of deflection of delaminated reinforces concrete composite floor based on assumed frictional – elastic model of composite surface*. AMCM' 2008 6th International Conference, June 9-11, Łódź, p. 219-220.

11. M. JAROSIŃSKA, *Damage detection in steel – concrete composite beams using modal analysis*. Research and Analyses of the Selected problems of Construction. Silesian University of Technology Editions, p. 555-563, 2011.

12. W.J. PALM, *Mechanical vibration*, John Wiley & Sons, Inc 2006.

13. D.J. INMAN, *Engineering vibration*, Pearson, 2008.

14. Z. OSIŃSKI, *Dumping of mechanical vibrations* [in Polish], PWN 1979.

15. Z. OSIŃSKI, *Vibration dumping* [in Polish], PWN 1997.

16. W. DERSKI, S. ZIEMBA, *Analysis of reological models* [in Polish], Institute of the Basic Technological Problems of the PAN. Warszawa 1968.

17. I. BRONSZTEJN, N. SIEMIENEDIAJEW, G. MUSIOŁ, H. MÜHLIG, *Modern compendium of mathematics* [in Polish], PWN 2004.

MODELOWANIE WPŁYWU SZTYWNOŚCI ZESPOLENIA NA ROZPRASZANIE ENERGII W WARSTWIE KONTAKTOWEJ ŻELBETOWYCH STROPÓW ZESPOLONYCH

S t r e s z c z e n i e

Żelbetowe stropy zespolone składają się z dwóch warstw betonu: dolnej stanowiącej element prefabrykowany oraz górnej wykonywanej na budowie. Przyjęto, że między tymi warstwami znajduje się warstwa kontaktowa, w której wywoływane są siły związane z odkształceniami sprężystymi oraz niesprężystymi.

Zdefiniowano model ciała reprezentującego warstwę kontaktową przyjmując że występują w nim naprężenia liniowo-sprężyste i niesprężyste związane z tarciem wewnątrz materiałowym.

Następnie zbudowano model żelbetowego stropu zespolonego o jednym stopniu swobody. Model ten składa z dwóch połączonych szeregowo modeli o jednym stopniu swobody: płyty monolitycznej i elementu reprezentującego liniowo-sprężyste i niesprężyste właściwości warstwy kontaktowej.

Niesprężyste właściwości w modelu, przy statycznym wymuszeniu kinematycznym były reprezentowane przez elementy sprężysto-tarciowe. Przy wymuszeniu kinematycznym tłumienie modelowano elementami wiskotycznymi. Z fizycznego punktu widzenia rozważano sytuację, w której występują ciągłe odkształcenia w warstwie kontaktowej, to znaczy nie zachodzi poślizg między betonem warstwy dolnej i górnej.

Badania modelu wykazały, że w procesie statycznego obciążania i odciążania modelu płyty zespolonej powstaje pętla histerezy, która pozwala wyznaczać wartości współczynnika pochłaniania energii przy statycznym wymuszeniu kinematycznym. Mniejszymi wartościami tego współczynnika cechują się modele o małej sprężystości zespolenia.

W zdefiniowanym modelu przyjęto, że w trakcie drgań, niesprężyste siły tarcia wewnętrznego w zespoleniu oraz w betonie warstw dolnej i górnej ujawniają się w postaci tarcia wiskotycznego. Wykazano, że drgania modeli płyt zespolonych cechujących się małą sztywnością odpowiadającą zespoleniu są tłumione mocniej niż drgania modeli płyt ze sztywną warstwą kontaktową. Ponadto mniejszej sztywności warstwy kontaktowej odpowiada mniejsza częstotliwości drgań własnych modeli płyt.

Powyższe spostrzeżenia dotyczące dyssypacji energii w czasie statycznego i dynamicznego obciążania zdefiniowanych modeli płyt mają duże znaczenie praktyczne, ponieważ, po ich praktycznym zweryfikowaniu, umożliwią określanie sztywności zespolenia dwóch betonów w zespolonych stropach deskowych. Jak wykazano bowiem we wcześniejszych badaniach doświadczalnych, płyty o małej sztywności zespolenia pod mniejszym obciążeniem osiągają graniczną wartość przemieszczenia i utracie ich nośności towarzyszy rozwarstwienie.

Wyniki przeprowadzonych analiz teoretycznych są jedną z podstaw prowadzonych aktualnie badań doświadczalnych, w których bada się dyssypację energii w żelbetowych stropach deskowych poddanych wymuszeniom kinematycznym statycznym i dynamicznym.